Supplemental Material

Supplemental Experimental Procedures

Detailed description of cellular models and culture conditions used in this study **(Figure S10):**

EpH4, a murine mammary epithelial cell line spontaneously immortalized from mid-pregnant mice, undergoes complete epithelial polarization in cell culture, either on porous supports or in serum-free 3D collagen-I gels, where these cells form organotypic, tubular structures. TGFβ treatment causes cell cycle arrest and apoptosis in EpH4 (Grunert et al, 2003; Huber et al, 2005) cells. After transformation with oncogenic Ha-RasV12 – which hyperactivates both the MAPK-and PI3K pathways – the resulting ***EpRas*** cells remain largely epithelial and form alveolar structures with larger lumina in collagen gels, and also show increased proliferation (Grunert et al, 2003; Janda et al, 2002a; Oft et al, 1996). Upon TGFβ treatment, ***EpRas*** cells undergo **EMT** in collagen gels, leading to a fibroblastoid morphology, high motility and invasive growth within collagen gels. The resulting ***EpRasXT*** cells show loss of epithelial markers (E-cadherin, ZO-1) and upregulation of mesenchymal markers i.e Vimentin and Fibronectin (Grunert et al, 2003; Yang et al, 2004). EpRas and EpRasXT cells cause large tumors showing EMT *in vivo* after subcutaneous or mammary gland fat pad injection, and induce strong lung metastasis in nude mice upon tail vein injection, indicating that the cells perform late (extravasation) but not early steps of metastasis (e.g. intravasation (Grunert et al, 2003; Janda et al, 2002a; Oft et al, 1996; Waerner et al, 2006). EpH4 cells expressing a Ras effector domain mutant exclusively hyperactivating the PI3K pathway (***EpC40***) do not undergo TGFβ-induced EMT, but show only reversible loss of epithelial polarization, termed “scattering” (***EpC40XT***). These cells require TGFβ to maintain their fibroblastoid phenotype with persisting plasma membrane-E-cadherin- and no Vimentin expression (Janda et al, 2002a; Janda et al, 2002b). They are protected from TGFβ-induced apoptosis due to enhanced PI3K activation and form tumors in nude mice, but neither undergo EMT in the tumors nor form lung metastases upon tail vein injection (Janda et al, 2002b).

EpH4 cells after forced expression of c-FosER (***EpFosER***) – an estrogen-inducible fusion protein of c-Fos and the hormone-binding domain of the estrogen receptor – can be induced to undergo stable, irreversible EMT by long-term cultivation in the presence of estradiol (***mesFosER***;

Eger et al, 2000; Reichmann et al, 1992). Stable knockdown of AnxA1 in EpRas and EpC40 cells yielded ***EpRas-siAnxA1*** and ***EpC40-siAnxA1*** cells, which showed a similar, fibroblastoid EMT-phenotype as EpRasXT cells (Figs. S10B-1,B-2). All EpH4-derived cells were cultivated in DMEM/F12 medium (GIBCO) plus 10% fetal bovine serum (FCS), 100 U/ml penicillin and 50µg/ml streptomycin, 1mM HEPES, 2mM L-glutamine. However, for cultivation of EpRas cells FCS was reduced to 4%, while EpRasXT cells were kept in medium with 15%FCS. To guarantee similar culture conditions of all cells used to produce culture supernatants for analysis of secreted factors, cells were cultivated overnight in media without serum and supernatants concentrated by ultrafiltration.

As a control experiment for potential off-target effects of AnxA1 knockdown in EpC40 cells, we retrovirally expressed full-length human AnxA1 cDNA in EpC40-siAnxA1 cells using a GFP-containing retroviral vector. GFP positive ***EpC40-siAnxA1+hAnxA1*** cells showed enhanced AnxA1 expression (Fig. S2C) and were reversed to an epithelial phenotype (Fig. S2C, D).

The **human mammary carcinoma cell lines** BT474, MCF7, T47D, ZR751, SKBR3, HS578T and MDA-MB-231 (Fig. S10A-4) are described in detail in (Eger et al, 2005). While BT474, MCF7 and T47D form a cobblestone-like, epitheloid monolayer on plastic, express E-cadherin and lack the E-cadherin repressor deltaEF1, the cell lines SKBR3, HS578T and MDA-MB-231 have fibroblastoid morphology, lack E-cadherin and express high levels of deltaEF1. The cell line ZR751 grows in clumps of rounded cells with low adherence, but expresses E-cadherin and lacks deltaEF1 (Eger et al, 2005). These cells were grown in the same medium as EpH4 cells. The cell lines ***MDA-MB-231-empty*** and ***MDA-MB-231+AnxA1*** were cultivated in medium containing 4%FCS.

Various ***HMEC-derivatives***, kindly provided by Dr. William Hahn (Zhao et al, 2003), were grown in a special, serum-free medium (human mammary epithelial cell growth medium containing a supplement mix; MEGM, Promocell). The *HMEC*-derivatives used expressed SV40 large T (LT) plus SV40 small T (sT) (***HMEC-hTert/LT/sT***), oncogenic HaRas plus SV40 large T (***HMEC-hTert/Ras/LT***) or co-expressed all three oncogenes (***HMEC-hTert/Ras/LT/sT***), respectively.

The ***MDCK-DDRafER*** cell line, originally obtained from J. Downward (Lehmann et al, 2000) was optimized by cloning to resemble the original, fully polarized MDCK cells in absence of

ligands (Tanos & Rodriguez-Boulan, 2008). Cells were grown in DMEM/F12 plus 10% FCS. For EMT-induction, the cells were seeded and maintained on plastic at semi-confluent density and treated or not treated with $3x10^{-6}$ M estradiol (E2) for 2 days. Cells were then trypsinized, re-seeded at near confluency on porous supports (translucent filters with 1.5 µm mean pore size, 1.7 or 4.5 cm in diameter) and treated or not treated with E2 plus 3ng/ml TGFβ1 for 4-5 days, during which time untreated cells got dense enough to fully polarize (as shown with apical markers and Z-stack analysis, not shown). Treatment with drugs or inhibitors was performed while the cells were expanding for 4-5 days on filters.

Tissue collections and databases used for analysis of endogenous AnxA1 levels:

Human breast cancer tissue samples (Fig. S10A-6) were obtained from the Biobank of the Medical University Graz, Department of Pathology, as a kind gift of Dr. Kurt Zatloukal. All tissues were snap-frozen in methylbutane pre-cooled with liquid nitrogen within 20min after surgery. The study was approved by the ethical committee of the Medical University Graz. RNA was prepared from these tissue samples according to standard procedures and processed for quantitative RT-PCR (qRT-PCR) as described in the main text and below. The samples consisted of 4 benign mammary tissue samples and 20 samples from invasive breast tumors.

Analysis of the ***Gene Logic database*** for AnxA1 expression in normal and cancerous breast, colon and lung tissues (Fig. S10A-5) was performed by Boehringer Ingelheim Austria (BI Austria) personnel (Ferby et al, 2006), who provided us with the graph in Fig. S1A, which depicts data from evaluating Affymetrics chips containing probes for essentially all human genes and hybridized with probes from >10 different human carcinoma types prepared from 20 to >100 tissue samples from cancer patients as well as normal tissues. The data shown in Fig. S1A are derived from the following numbers of tissues: Breast carcinoma: 86 tumors, 89 normal tissues; Lung (NSC; non small cell) carcinoma: 19 tumors, 106 normal tissues; Prostate carcinoma: 51 tumors, 21 normal tissues. The following data are depicted within the graph of Fig. S1A: mean expression levels, vertical line within coloured blocks; standard deviation, length of coloured blocks; range of expression levels, horizontal bars; high and low extremes not included into evaluation, small circles.

Retroviral vectors causing stable AnxA1-knockdown: Oligonucleotides and vector generation:

All procedures were performed according to Gateway protocol's instructions (Invitrogen). The following two different oligonucleotides were selected for RNAi of murine AnxA1:

5´AGGGTAGGGGCTCACTGCTGACCCAGGA3`

5´GGAGACCATAAT CCTGATCAATGCCTTA3`,

annealed with respective, second oligonucleotides and the resulting, double-stranded shRNA fragments were inserted into the gateway-compatible pSHAG vector (Paddison et al, 2002) according to the Gateway protocol's instructions (Invitrogen). The resulting U6-promoter-driven shRNAs were then transferred to the pMSCV-pgk-puromycin retroviral vector (Clontech) by recombination, according to Gateway protocols instructions. A basic BLAST alignment search of all target sequences did not reveal significant sequence homology with other genes. All shRNA-expressing vectors were confirmed by sequence analysis of the target insert. Vectors containing 28nt target sequence for human AnxA1 were generated as described above for the mouse constructs, selecting three oligonucleotide sequences:

5´GAATGGTATCAGAATTCCTCAAGCAGGC3´,

5`AGACATTAACAGGGTCTACAGAGAGGAA3`,

5`CCTACCTTCAATCCATCCTCGGATGTCG3.

To generate retroviral vectors expressing human AnxA1, we PCR-amplified full length AnxA1 from a cDNA library. This DNA was inserted into the p201 gateway donor vector and then subcloned into two different target vectors by recombination according to the gateway protocol (Invitrogen): the pMSCV-pgk-puromycin vector to infect MDA-MB-231 cells and the pMSCV-GFP target vector to infect the already puro-resistant EpC40-siAnxA1 cells. The insert was confirmed by sequencing using specific primers in both constructs.

Generation of stable cell lines expressing the above retroviral vector:

Retrovirus producer cell lines (NIH-3T3gp+86 cells) were transfected with the above retroviral constructs using Lipofectamine2000 reagent (Invitrogen). These producer cells were seeded into 6-well plates (4.5 ml medium) at densities allowing generation of semiconfluent cell layers at three consecutive days. Twice daily, supernatants were harvested from producer cells having the correct density, filtered through a 0.45 µm filter and used to infect target cells in the presence of polybrene (2µg/ml) by respective medium changes. Cells were then selected for 2

weeks with 2.5µg/ml Puromycin or were FACS sorted for GFP-positive cells and the resulting pools tested for reduction (AnxA1-RNAi) or elevation (exogenous expression of AnxA1) by Western Blot analysis. Pools with significant AnxA1 knockdown (obtained from vectors harboring different AnxA1-specific siRNAs) or AnxA1 overexpression were cloned via single-cell FACS-sorting into 96-well plates, expanded clones were verified by Western Blot analysis and frozen in liquid nitrogen. Stable knock down clones of Jak1, Jak2 and Tyk2 were generated using MISSION Lentiviral Transduction particles (Sigma-Aldrich; Jak1: NM_146145; Jak2: NM_008413; Tyk2: NM_018793) according to the manufacturer's instruction. Briefly, 1,6 x 10^4 cells/well were seeded into 96 well plates in growth medium and grown to 50% confluency. 1-3 x 10^5 transduction units (TU) in presence of polybrene were added to the cells. Following 24hr incubation, the medium was changed and the cells were selected with puromycine. Unfortunately, normally proliferating knockdown clones obtained showed no strong reduction of the respective target mRNAs.

Antibodies and pharmacological inhibitors:

The following antibodies were used in Western Blot- and immunofluorescence analysis (Catalogue Nr's and working dilutions in brackets). Antibodies against EGFR (sc-31155 and sc-03; 1:1000), AnxA1 (sc-11387, 1:1000), AnxA5 (sc-8300; 1:1000), AnxA6 (sc-11388; 1:1000) and AnxA7 (sc-11389; 1:1000) were from Santa Cruz. Antibodies to AnxA2 (610068; 1:1000) and AnxA4 (610294; 1:1000) were from BD Transduction Laboratories. Antibody to N-cadherin (33-3900; 1:1000) was from Zymed and antibodies to Vimentin (V 5255; 1:500), β-actin (A 2066¸ 1:500), pErk1/2 (M 8159; 1: 40000) and total Erk1/2 (M 5670; 1:20000) were from Sigma. Antibodies to the total- and serine-phosphorylated proteins Stat3 (9132, 9135; 1:500), Smad2 (3102, 3101; 1:1000), AKT (9270, 9268; 1:1000), p38MAPK (9212, 9211; 1:1000) were from Cell Signaling. The E-cadherin antibody (610181; 1:1000) was from Becton Dickinson (BD). Phosphorylation of the EGFR was detected after immunoprecipitation with an EGFR specific antibody (sc-03), using the 4G10 antibody from Millipore (05-321; 1:1000). The TGFβ1 antibody was from Promega (G 1221; 1:500). The antibody used for detecting AnxA1 by immunofluorescence (1:500) and immunohistochemistry (IHC) (1:1500) was from Becton Dickinson (BD; 610067).

The pan-Jak inhibitor I (2µM, inhibiting Jak1, Jak2, Jak3 and Tyk2, but not EGFR, src or other RTKs), Mek-1 inhibitor (PD98.059; 20 µM), p38 MAPK inhibitor (SB202.190; 10 µM,) and PI3K-inhibitor (LY294.002; 20 µM) were from Calbiochem and Sigma, the Ras-inhibitor (L739.749; 10 µM), EGFR-inhibitor (H14; 5µM) and TGFβRI-inhibitor (SB431.542; 5-10 µM) were kind gifts from Boehringer Ingelheim International (BI). The Jak2- and Tyk2-specific inhibitors AG490 and AG1 were from Calbiochem. Salinomycin was from Sigma.

Most pharmacological inhibitors were used as 5-50 mM stock solutions in DMSO, stored at -80°C and added daily to cells in collagen gels – or porous supports in case of MDCK-DDRafER cells – starting 24 hours after cell seeding and avoiding > 1/1000 DMSO dilutions. Salinomycin was dissolved at a concentration of 50mM in Methanol. Powder and stock solutions of the Ras (farnesyl-transferase) inhibitor L739.749 were stored at -70ºC, dilutions were prepared immediately before addition to cells, kept on ice and made fresh every day. Inhibitor working concentrations leading to a complete response were determined earlier on cell types known to respond to the above inhibitors against p38MAPK (Maschler et al, 2004), PI3K, MEK, and RAS (Janda et al, 2002a; Janda et al, 2002b); TGFβRI (Waerner et al, 2006) and Jak inhibitor I (Grebien et al, 2008).

Detailed procedure for Western Blot analysis:

For Western Blot (WB) analysis, cells were lysed on ice for 20 min in ice-cold RIPA buffer, containing 150mM NaCl, 50mM Tris pH 7.4, 1% NP40, 1% Na-desoxycholate, 1mM Na_3VO_4, 25mM NaF, 1mM PMSF, 5mM β-glycerol-phosphate, 10mM DTT, protease inhibitor cocktail tablets (Complete mini; Roche, according to manufacturer`s instructions). Lysates were cleared for 5 min at 12500xg and 4°C and protein concentrations determined using the Bradford assay (Biorad). 40µg of protein were denatured in SDS-sample buffer, followed by SDS-PAGE and transferred to PVDF membranes. After treatment with blocking solution (5% bovine serum albumin (BSA) in TBST; i.e. Tris-buffered saline + Tween 20), membranes were incubated with the respective antibody in blocking solution for 1hr at room temperature or over night at 4°C, washed with plain TBST and incubated with the respective secondary antibody in blocking solution for 1hr at room temperature. After 5 washes with TBST for 30 min, the blots were developed using an enhanced chemiluminescence kit (ECL, Amersham). Quantitation of WB data from human breast carcinoma cells analysed for AnxA1 protein expression was performed by densitometry, using

ImageJ software according to the manufacturers instructions, using loading control data (β-actin) for normalization.

Immunoprecipitation of cell surface- and metabolically labelled proteins: detailed procedure:.

For exclusive ***labelling of cell surface proteins***, cell surface biotinylation was performed as described previously (Maschler et al, 2005) with minor modifications. Briefly, cells were detached by trypsinisation, washed in Hank`s balanced salt solution (HBSS) and biotinylated at $2x10^6$ cells per ml for 30 min, using 1mg/ml Sulfo-NHS-Biotin (Sigma) in HBSS. After stopping the biotinylation reaction with DMEM containing 0.6 % bovine serum albumin (BSA) for 10 min, cells were washed extensively in HBSS and lysed in 50mM Tris (pH 7.5), 0.1% Triton X100, 50mM NaCl. Equal amounts of protein were immunoprecipitated with the respective antibody for 1 hour and immune complexes collected using Protein A/G plus beads (Santa Cruz). The immunoprecipitates (removed from beads with SDS sample buffer) were subjected to SDS-PAGE, transferred to nitrocellulose membranes (Amersham) and incubated with blocking solution (see Western Blot) at 50°C for 1 hour. Biotinylated proteins were detected by treating the membrane with streptavidine-horse radish peroxidase (Sigma, 1:5000 in 1%BSA for 1hr at room temperature) and visualized using ECL-detection reagent.

For ***metabolic labelling***, equal cell numbers were plated on 10 cm plastic dishes in 10 ml medium at 1-3 $x10^6$ cells/dish and pre-incubated with methionine and cysteine-free MEM (GIBCO) for 1hr, then labelled with 100µCi of [^{35}S]-L-methionine/L-cysteine (MP Biomedicals) in 10 ml of the above medium for 5hr and lysed as described for Western blot analysis. Aliquots of cell lysates were cleared by centrifugation and aliquots containing 2 x 10^6 cpm of incorporated [^{35}S] were subjected to immunoprecipitation with appropriate antibodies. Precipitated proteins were subjected to SDS-PAGE. Gels were fixed in 7% acetic acid, 25% methanol in aqua dest. for 30 min, treated with ENHANCE amplifier solution (NEN), dried and exposed for autoradiography on Kodak X-ray film in enhancer screen cassettes.

Collagen gel culture methods and immunofluorescence analysis:

For successful 3D culture of MDA-MB-231 cells in collagen gels, we optimized the cell numbers seeded (between 1000 and 3000 cells per gel). TGFβ was added 2 days after seeding where indicated, while pharmacological inhibitors were added 1 day after seeding. Depending on

the growth rate of the collagen structures, gels were maintained for 7-10 days, after which they were photographed, fixed and processed for antibody staining.

Non-Permeant cellular ELISA: details and minor modifications:

Cell surface EGFR was determined using a non permeant cellular ELISA assay described in (Lee et al, 2002) with minor modifications. Briefly, $1x10^4$ cells were seeded into 12-well plates in 1.5 ml medium and cultivated for 24 hours. Cells were then fixed with 4% paraformaldehyde in 50mM phosphate buffer (pH 7.2) for 20min at room temperature. Cells were washed three times with ice cold PBS containing 0.1M glycine and incubated with 3% H_2O_2 in PBS for 5 minutes to minimize endogenous peroxidase activity. After blocking with 5%FCS+1% BSA in PBS for 30 minutes, cells were incubated for 1 hour at room temperature with the primary anti-EGFR-antibody (Santa Cruz, sc-03, 1µg/ml in blocking solution), subsequently washed three times with ice cold PBS and treated with the peroxidase conjugated secondary antibody. Then cells were washed and the colour reaction was carried out with the substrate solution of the IL6 ELISA kit. The coloured reaction end product was transferred to a microtiter plate and stop solution (from the IL6 ELISA kit) was added. After 30min, the colour reaction was measured with an ELISA reader at 450nm, using 570nm as the control wavelength.

Analysis of AnxA1 expression in human tissue tumor arrays by immunohistochemistry:

Slides bearing 3 µm sections from two human breast cancer tissue tumor arrays (TA2, TA3) using primary tumor tissue from 141 patients with known disease history were dried at 65°C for 45 minutes, deparaffinated by washing with xylene three times followed by incubation in 100% and 50% ethanol. Antigen retrieval was performed by incubating the slides in antigen retrieval buffer (DAKO S1699) for 30minutes at 95°C. After the slides were allowed to cool down they were washed once in 1xPBS and incubated in blocking solution (15% goat serum / PBS) for 15 minutes. Primary antibody (anti-AnxA1; Becton Dickinson; BD 610067) was added at a dilution of 1:1500 in 1%BSA / PBS and slides were incubated for 60 minutes. Endogenous peroxidase was blocked by treating the samples with 0.3% H_2O_2 / PBS for 20minutes. After washing 3 times with 1xPBS the secondary antibody (biotinylated, DAKO E0413) was added at a dilution of 1:500 in 1%BSA / PBS and the samples were incubated for 30minutes followed by three washing steps with PBS. The streptavidine-biotin complex (DAKO K0377) was added for 30 minutes. Then the slides were

washed three times in PBS and colour development was carried out in AEC (1% w/v 3,3-amino-9-ethyl-carbazole; Sigma 5754 in N, N-dimethylformamide). Counter-stain was performed with Hematoxylin (Sigma MHS-16). The slides were then washed in tap water, dried for 15minutes and mounted in mounting medium (Aquatex, Merck 1.08562) and analysed by high resolution imaging (MIRAX-software) of the stained arrays. After normalization of staining intensity using Adobe Photoshop CS4 (Waerner et al, 2006), using blue nuclear and cytoplasmic staining for normalization, intensity and subcellular localization of the brown AnxA1 signal was recorded and correlated in Kaplan-Meier plots to metastasis free survival and overall survival (Waerner et al, 2006), using the available patient disease history information.

RNA Isolation and cDNA synthesis:

Total RNA was isolated using the TRIzol Reagent (Invitrogen) according to the manufacturer's instruction. cDNA was synthesized from 2µg of total RNA using the "Ready to go you prime First Strand" beads kit (Amersham Biosciences) and random oligonucleotides according to the manufacturer`s instruction.

qRT-PCR of AnxA1 levels in cell lines and tumor tissues:

RNA was prepared from cell pellets containing 1-2x10^8 cells or from tumor tissues according to standard procedures. qRT-PCR of the expression levels of AnxA1 in these RNA samples was performed using the SYBR green 2x PCR kit (Applied Biosciences) and a primer mix from Qiagen and were normalized to GAPDH levels.

qRT-PCR of E-cadherin repressor in cell lines:

1µl of cDNA was used per reaction, which was performed using SYBR Green (Molecular Probes) and an Opticon2 Monitor Fluorescence Thermocycler in a 25µl reaction volume for 40 cycles. Comparable Ct (cycle threshold) method was used to quantify the amplified fragments and RNA expression levels were normalized to GAPDH.

Tumor formation and metastasis assay: minor modifications and details*:*

Tumor formation ability was determined by mammary gland fat pad or subcutanous injection as described earlier (Jechlinger et al, 2002; Maschler et al, 2005; Zhao et al, 2003), with minor modifications. Briefly, cells to be injected were trypsinized, washed in PBS and 1x10^5 cells were

injected into the mammary gland fat pad of anesthetized MF1 nu/nu mice (2 injection sites per mouse, 3 mice each). For subcutaneous injection of cells from the HMEC cell series described above, trypsinized cells were washed with PBS and $4x10^6$ cells were injected in 0.1 ml PBS (4 injection sites per mouse, 2 mice per cell line). In the subcutaneously injected mice receiving the HMEC-series, tumors occurred after approximately 4 weeks. Tumor weight was measured by dissecting out the tumor and determining tumor weight, by immersing tumors into PBS-filled, pre-weighed dishes and weighing them again.

Metastasis formation was measured after injection of the respective cell lines into the tail vein of nude mice (Janda et al, 2002a; Waerner et al, 2006). $1x10^5$ cells in 0.1ml of PBS were injected into the tail vein of MF1 nu/nu mice, using 3 mice per cell type with MDA-MB231-control, MDA-MB231+AnxA1, EpRas-sicontrol, and EpRas-siAnxA1 cells and 7 mice per cell type for EpC40-sicontrol and EpC40-siAnxA1 cells. Mice were inspected every few days and sacrificed when becoming moribund, which occurred between 25 and 45 days in the mice injected with EpC40-siAnxA1 and MDAMB231-control vector cells, while the lungs remained metastasis-free for >100 days with EpC40-sicontrol cells and for >55 days in case of the MDA-MB-231+AnxA1 cells. Two experiments were done with three and four mice injected with EpC40-sicontrol, and EpC40-siAnxA1 cells (using the AnxA1/2 and AnxA1/6 cell clones) and pooling the data in Fig. 3f, the observation times of the control mice in these two experiments were 16 and 12 weeks. In case of the EpRas-sicontrol and EpRas-siAnxA1 cells, the latter formed already large metastases at a time where the control EpRas cells had just started to form tiny metastases. Due to these “black and white” differences in the first two models, metastases were only counted on the surface of the dissected lungs immersed in PBS under a dissection microscope, rather than counting metastases in serial sections.

Supplemental Material: AnxA1 expression in various human tumors (summary of published data; focus on metastasis)

AnxA1 was downregulated in breast cancer (Shen et al, 2005; Shen et al, 2006), thyroid cancer (Petrella et al, 2006), head and neck cancer (Garcia Pedrero et al, 2004), larynx tumors (Silistino-Souza et al, 2007) and nasopharyngeal carcinomas (Rodrigo et al, 2005). In contrast, AnxA1 was upregulated in early stage human skin tumors (Hummerich et al, 2006), esophageal

adenocarcinomas (Wang et al, 2006b), intrahepatic cholangiocarcinomas (Wang et al, 2006a) astrocytomas (Ruano et al, 2008) and renal cell carcinomas (Zimmermann et al, 2007). Although not discussed by the respective authors, high AnxA1-expression was typical for early stage cancers like adenomas in most reports, while loss of AnxA1 was mainly seen in more strongly progressed tumors (Lim & Pervaiz, 2007; Mussunoor & Murray, 2008). Importantly, however, very little has been published on AnxA1-expression during metastasis, particularly with respect to tumor cells at the invasion front, which (often transiently) lose epithelial polarity and gain EMT. In addition, the subcellular localization of AnxA1 – changing from cytoplasmic- to vesicle- localization during butyrate- or inosine-induced colon carcinoma epithelial differentiation (Guzman-Aranguez et al, 2005), and between plasma-membrane- and cytoplasmic localization in renal cell carcinomas (Zimmermann et al, 2007) – might also contribute to tumor progression.

Another reason for the varying role of AnxA1 overexpression versus loss in different tumor types is that its function in cells greatly varies with respect to coexpression of oncogenic Ras. We showed that loss of AnxA1 is badly tolerated in cells lacking oncogenic Ras, while it causes EMT in cells expressing oncogenic Ras (this paper and unpublished). Since many tumor types depend on increased Ras- or Raf-expression, while others do not, this may add to the explanation of the variable behavior of tumor cells overexpressing or lacking AnxA1.

Supplemental Material*:* Experiments with Transgenic mice

FVB/N-TgN(MMTV-*neu*)202Mul (stock no. 002376) and FVB/NJ-Tg(MMTV-*TGFβ1*) 46Hlm/J (stock no.002933) mice were obtained from Jackson Laboratories. Heterozygous FVB/NJ-Tg(MMTV-*TGFβ1* x MMTV-*Neu*) mice were generated from the above strains by respective breeding. Female mice from FVB/N-TgN(MMTV-*neu*) and FVB/NJ-Tg(MMTV-*TGFβ1* x MMTV-*Neu*) were maintained separated from males until tumors developed (6-9 months). Tumors were snap frozen in liquid nitrogen and kept at -80°C. For histology and expression of EMT-markers in these tumors, see (Jechlinger et al, 2006). For Western Blot analysis, small tumor pieces were lysed in RIPA buffer using a homogenizer and lysates were then subjected to SDS-PAGE (see main text, Fig. 1E).

To test, whether or not loss of AnxA1 would enhance metastasis in an *in vivo* metastasis mouse model, we used 129/Bl6-Annexin A1-/- mice (kindly provided by R.Flowers, London, GB)

and wt mice of the same mixed background. These mice were crossbred to the abovementioned MMTV-*neu*- or MMTV-*neu* x MMTV-*TGFβ* transgenic mice to generate these strains on a AnxA1-/- background. During an observation time of >1.2 years, these mice developed tumors and metastases at similar ages as the two respective FVB/N-transgenic strains not bred to AnxA1-/- mice, indicating that *neu* was not sufficient to enhance metastasis in AnxA1-/- mice which show early compensation by other family members. In line with this, EpH4 cell expressing activated HER2* underwent reversible rather than metastable EMT upon exposure to TGFβ (A. Pacher and HB, unpublished), suggesting that HER2* in contrast to oncogenic Ras cannot sustain a complete EMT phenotype.

Supplemental Material: In vivo experiment with HMEC-derived, oncogene-containing cell lines before and after siRNA-mediated human AnxA1 knockdown

Since AnxA1-RNAi also stimulated tumor growth (Fig. 3A, C), we tested whether loss of AnxA1 would induce tumorigenicity in hTERT-immortalized human mammary epithelial cells (HMEC) expressing defined oncogenes (Hahn et al, 2002), i.e. exogenous, oncogenic RasV12, SV40 small T (sT) and/or SV40-large T (LT). We knocked down AnxA1 in non-tumorigenic HMEC/hTERT, LT, sT and HMEC/hTERT, LT, RasV12 and tested tumor formation of these cells by subcutaneous injection into nude mice. Tumorigenic HMEC/hTERT, LT, sT, RasV12 cells were used as positive controls (Fig. S3B). AnxA1 knockdown rendered HMEC/hTERT, LT, RasV12 tumorigenic, but was ineffective in HMEC/hTERT, LT, sT (Fig. S3B), suggesting that AnxA1 might replace the PP2A- or PI3K-signalling activities of SV40-sT (Zhao et al, 2003), but not oncogenic Ras.

Supplemental References

Eger A, Aigner K, Sonderegger S, Dampier B, Oehler S, Schreiber M, Berx G, Cano A, Beug H, Foisner R (2005). DeltaEF1 is a transcriptional repressor of E-cadherin and regulates epithelial plasticity in breast cancer cells. *Oncogene*, **24**, 2375-2385

Eger A, Stockinger A, Schaffhauser B, Beug H, Foisner R (2000). Epithelial mesenchymal

transition by c-Fos estrogen receptor activation involves nuclear translocation of beta-catenin and upregulation of beta-catenin/lymphoid enhancer binding factor-1 transcriptional activity. *J. Cell Biol.*, **148**, 173-188

Ferby I, Reschke M, Kudlacek O, Pante G, Amann K, Sommergruber W, Kraut N, Ullrich A, Fassler R, Klein R (2006). Mig6 is a negative regulator of EGF receptor–mediated skin morphogenesis and tumor formation. *Nat. Med.*, **12**, 568-573

Garcia Pedrero JM, Fernandez MP, Morgan RO, Herrero Zapatero A, Gonzalez MV, Suarez Nieto C, Rodrigo JP (2004). Annexin A1 down-regulation in head and neck cancer is associated with epithelial differentiation status. *Am. J. Pathol.*, **164**, 73-79

Grebien F, Kerenyi MA, Kovacic B, Kolbe T, Becker V, Dolznig H, Pfeffer K, Klingmueller U, Mueller M, Beug, Mueller EW, Moriggl R (2008). Stat5 activation enables erythropoiesis in the absence of EpoR and Jak2. *Blood*, **111**, 4511-4522

Grunert S, Jechlinger M, Beug H (2003). Diverse cellular and molecular mechanisms contribute to epithelial plasticity and metastasis. *Nat. Rev. Mol. Cell Biol.*, **4**, 657-665

Guzman-Aranguez A, Olmo N, Turnay J, Lecona E, Perez-Ramos P, Lopez de Silanes I, Lizarbe MA(2005). Differentiation of human colon adenocarcinoma cells alters the expression and intracellular localization of annexins A1, A2, and A5. *J. Cell. Biochem.*, **94**, 178-193

Hahn WC, Dessain SK, Brooks MW, King JE, Elenbaas B, Sabatini DM, DeCaprio JA, Weinberg RA (2002). Enumeration of the simian virus 40 early region elements necessary for human cell transformation. *Mol. Cell Biol.*, **22**, 2111-2123

Huber MA, Kraut N Beug H (2005). Molecular Requirements for Epithelial-Mesenchymal Transition During Tumor Progression. *Curr. Opin. Cell Biol.*, **17**, 548-558

Hummerich L, Muller R, Hess J, Kokocinski F, Hahn M, Furstenberger G, Mauch C, Lichter P, Angle P (2006). Identification of novel tumour-associated genes differentially expressed in the process of squamous cell cancer development. *Oncogene*, **25**, 111-121

Janda E, Lehmann K, Killisch I, Jechlinger M, Herzig M, Downward J Beug H, Grunert S (2002a). Ras and TGF[beta] cooperatively regulate epithelial cell plasticity and metastasis: dissection of Ras signaling pathways. *J. Cell. Biol.*, **156**, 299-313.

Janda E, Litos G, Grunert S, Downward J, Beug, H (2002b). Oncogenic Ras/Her-2 mediate hyperproliferation of polarized epithelial cells in 3D cultures and rapid tumor growth via the PI3K pathway. *Oncogene*, **21**, 5148-5159

Jechlinger M, Grunert S, Beug H (2002). Mechanisms in epithelial plasticity and metastasis: insights from 3D cultures and expression profiling. *J. Mammary Gland Biol. Neoplasia*, **7**, 415-432

Jechlinger M, Sommer A, Moriggl R, Seither P, Kraut N, Capodiecci P, Donovan M, Cordon-Cardo C, Beug H, Grunert S (2006). Autocrine PDGFR signaling promotes mammary cancer metastasis. *J. Clin. Invest.*, **116**, 1561-1570

Lee FJ, Xue S, Pei L, Vukusic B, Chery N, Wang Y, Wang YT, Niznik HB, Yu XM, Liu F (2002). Dual regulation of NMDA receptor functions by direct protein-protein interactions with the dopamine D1 receptor. *Cell*, **111**, 219-230

Lehmann K, Janda E, Pierreux CE, Rytomaa M, Schulze A, McMahon M, Hill CS, Beug H, Downward J (2000) Raf induces TGFbeta production while blocking its apoptotic but not invasive responses: a mechanism leading to increased malignancy in epithelial cells. *Genes Dev* 14: 2610-2622.

Lim LH and Pervaiz S (2007). Annexin 1: the new face of an old molecule. *Faseb J.*, **21**, 968-975

Maschler S, Grunert S, Danielopol A, Beug H, Wirl G. (2004). Enhanced tenascin-C expression and matrix deposition during Ras/TGF-beta-induced progression of mammary tumor cells. *Oncogene*, **23**, 3622-3633

Maschler S, Wirl G, Spring H, Bredow DV, Sordat I, Beug H, Reichmann E (2005). Tumor cell

invasiveness correlates with changes in integrin expression and localization. *Oncogene*, **24**, 2032-2041

Mussunoor S and Murray GI (2008). The role of annexins in tumour development and progression. *J. Pathol.*, **216**, 131-140

Oft M, Peli J, Rudaz C, Schwarz H, Beug H, Reichmann E (1996). TGF-beta1 and Ha-Ras collaborate in modulating the phenotypic plasticity and invasiveness of epithelial tumor cells. *Genes Dev.*, **10**, 2462-2477

Paddison PJ, Caudy AA, Bernstein E, Hannon GJ, Conklin DS (2002). Short hairpin RNAs (shRNAs) induce sequence-specific silencing in mammalian cells. *Genes Dev.*, **16**, 948-958

Petrella A, Festa M, Ercolino SF, Zerilli M, Stassi G, Solito E, Parente L (2006). Annexin-1 downregulation in thyroid cancer correlates to the degree of tumor differentiation. *Cancer Biol. Ther.*, **5**, 643-647

Reichmann E, Schwarz H, Deiner EM, Leitner I, Eilers M, Berger J, Busslinger M, Beug H (1992). Activation of an inducible c-FosER fusion protein causes loss of epithelial polarity and triggers epithelial-fibroblastoid cell conversion. *Cell*, 71, 1103-16

Rodrigo JP, Garcia-Pedrero JM, Fernandez MP, Morgan RO, Suarez C, Herrero A (2005). Annexin A1 expression in nasopharyngeal carcinoma correlates with squamous differentiation. *Am. J. Rhinol.*, **19**, 483-487

Ruano Y, Mollejo M, Camacho FI, de Lope AR, Fiano C, Ribalta T Martinez P, Hernandez-Moneo JL, Melendez B (2008). Identification of survival-related genes of the phosphatidylinositol 3'-kinase signaling pathway in glioblastoma multiforme. *Cancer*, **112**, 1575-1584

Shen D, Chang HR, Chen Z, He J, Lonsberry V, Elshimali Y, Chia D, Seligson D, Goodglick N, Nelson SF, Gornbein JA (2005). Loss of annexin A1 expression in human breast cancer detected by multiple high-throughput analyses. *Biochem. Biophys. Res. Commun.*, **326**, 218-227

Shen D, Nooraie F, Elshimali Y, Lonsberry V, He J, Bose S, Chia D, Seligson D, Chang HR, Goodglick L (2006). Decreased expression of annexin A1 is correlated with breast cancer development and progression as determined by a tissue microarray analysis. *Hum. Pathol.*, **37**, 1583-1591

Silistino-Souza R, Rodrigues-Lisoni FC, Cury PM, Maniglia JV, Raposo LS, Tajara EH, Christian HC, Oliani SM (2007). Annexin 1: differential expression in tumor and mast cells in human larynx cancer. *Int. J. Cancer*, **120**, 2582-2589

Tanos B, Rodriguez-Boulan E (2008) The epithelial polarity program: machineries involved and their hijacking by cancer. *Oncogene* 27: 6939-6957

Waerner T, Alacakaptan M, Tamir I, Oberauer R, Gal A, Brabletz T, Schreiber M, Jechlinger M, Beug H (2006). ILEI: a cytokine essential for EMT, tumor formation, and late events in metastasis in epithelial cells. *Cancer Cell*, **10**, 227-239

Wang AG, Yoon SY, Oh JH, Jeon YJ, Kim M, Kim JM, Byun SS, Yang JO, Kim JH, Kim DG, Yeom Yi, Yoo HS, Kim YS, Kim NS (2006a). Identification of intrahepatic cholangiocarcinoma related genes by comparison with normal liver tissues using expressed sequence tags. *Biochem. Biophys. Res. Commun.*, **345**, 1022-1032

Wang KL, Wu TT, Resetkova E, Wang H, Correa AM, Hofstetter WL, Swisher SG, Ajani JA, Rashid A, Hamilton SR, Albarracin CT (2006b). Expression of annexin A1 in esophageal and esophagogastric junction adenocarcinomas: association with poor outcome. *Clin. Cancer Res.*, **12**, 4598-4604

Yang J, Mani SA, Donaher JL, Ramaswamy S, Itzykson RA, Come C, Savanger P, Gitelman I, Richardson A, Weinberg RA (2004). Twist, a master regulator of morphogenesis, plays an essential role in tumor metastasis. *Cell*, **117**, 927-939

Zhao JJ, Gjoerup OV, Subramanian RR, Cheng Y, Chen W, Roberts TM, HahnWC (2003). Human mammary epithelial cell transformation through the activation of phosphatidylinositol 3-

kinase. *Cancer Cell*, **3**, 483-495

Zimmermann U, Woenckhaus C, Teller S, Venz S, Langheinrich M, Protzel C Maile S, Junker H, Giebel J (2007). Expression of annexin AI in conventional renal cell carcinoma (CRCC) correlates with tumour stage, Fuhrman grade, amount of eosinophilic cells and clinical outcome. *Histol. Histopathol.*, **22**, 527-5349

Supplemental Figure Legends

Supplemental Figure S1: ***AnxA1 expression in various types of human carcinomas***

A) AnxA1 mRNA levels in 20-80 human breast-, lung- and prostate carcinoma samples (red) compared to similar numbers of respective normal tissue samples (green), data obtained from the Gene Logic Affymetrix chip database (see Suppl. Exp. Proc.). Data are depicted as follows: Vertical line within coloured blocks, mean expression levels; length of coloured blocks, standard deviation; horizontal bars, range of expression levels; small circles, high and low extreme values not included into the evaluation. *, significant difference ($p < 0.05$). **B)** Tissue samples from invasive mammary tumors (blue) and benign mammary tissue (green) were processed for qRT-PCR. Top, estrogen receptor (ER) and progesterone receptor (PR) status of the 20 tumors analysed. Error bars: S.D. from three independent determinations. Further details to (**A**) and (**B**): see Suppl. Exp. Proc. and Fig. S10A-5, 6.

Supplemental Figure S2: ***Specificity of the AnxA1 knockdown and complete reversal of EpRasXT cells by forced expression of human AnxA1***

A) Western blot (WB) analysis of EpH4, EpRas and EpRasXT cells (Fig. S10A-1), using antibodies to 6 different annexin family members. EpRasXT cells specifically lose AnxA1 expression while expression of the other annexins was unaltered during EMT. **B)** Lysates from EpRas cells before and after knockdown of AnxA1 (for phenotypes, see main text, Fig. 2B) were analyzed by WB for other annexin family members. Note that siRNA-mediated knockdown of

AnxA1 does not affect the expression level of 5 other annexins. **C)**, **D)** EpC40-siAnxA1 cells were infected with a human AnxA1-GFP- or an empty GFP-control vector, as shown by WB for GFP protein (**C**). Human AnxA1 restored E-cadherin- and suppressed Vimentin expression in EpC40-siAnxA1 cells shown by WB analysis (**C**), using β-actin as a loading control. **D)** Phase contrast microscopy of these cells on plastic (bar 20 µm) showed a clear fibroblastoid phenotype in the empty vector controls, while human AnxA1 re-expression reversed them to a cobblestone-like epithelial morphology. **E)** WB analysis of EpRasXT cells after forced expression of human AnxA1 showed re-induction of E-cadherin expression and loss of Vimentin and (**F**) reverted them to a cobblestone morphology on filters, which re-expressed plasma-membrane E-cadherin but completely lost Vimentin expression.

Supplemental Figure S3: ***AnxA1 knockdown plus oncogenic Ras causes tumors and metastasis***

A) Images of lungs photographed after dissection from mice 15 days after tail-vein injection of EpRas-sicontrol and EpRas-siAnxA1 cells. Note that the control cells have just started to form tiny metastases (white arrowheads), while the EpRas-siAnxA1 cells have already formed big metastases (red arrows). **B)** Tumor forming ability of HMEC-based cell lines expressing the shown combinations of known oncogenes before and after knockdown of AnxA1. Shown is a summary table of the data and an image of a representative mouse photographed 11 days after injection of HMEC-hTERT/Ras/LT/siAnxA1 cells. In all injected mice, different shRNA constructs targeting human AnxA1 caused sufficient AnxA1 knockdown to confer tumorigenicity. Control: HMECs expressing sicontrol vector. Note that knockdown of AnxA1 conferred tumorigenicity only in the presence of Ras, substituting for sT but not for Ras.

Supplemental Figure S4: ***Properties of EpC40-siAnxA1 cells recultivated from lung metastases, and resistance of EMT in MDA-MB-231 cells to treatment with pharmacological inhibitors***

A), **B)** Puromycin-resistant cells recultivated from metastases dissected from mouse lungs after tail vein injection of EpC40-siAnxA1 cells retain their low AnxA1 protein levels (**A**) and retain their fibroblastoid phenotype (**B**, bar, 20 µm). **C)** Images of MDA-MB-231 cells cultivated in collagen gels and treated or not treated with pharmacological inhibitors are shown (Bar, 50 µm). These cells – exhibiting a fibroblastoid phenotype (control) and expressing typical EMT-markers (see main text, Fig. 4A-C) – showed no or little response to various pharmacological inhibitors of

signalling pathways relevant to EMT. Inhibition of the Stat3 signalling pathway by the pan Jak-inhibitor-I retarded cell proliferation in the gels (inset), but did not abolish the fibroblastoid phenotype.

Supplemental Figure S5: ***Responses of EMT-associated signalling pathways to AnxA1-RNA and effects of respective pharmacological inhibitors on EpC40-siAnxA1 cells***

A) WB analysis of activated and total AKT (PI3K signalling), Erk1/2 and p38MAPK in EpRas- and EpC40 cells before and after siRNA-mediated AnxA1 knockdown. Note induction of pErk1/2 and pp38MAPK but not pAKT upon AnxA1 knockdown. **B)** Shown are bright field- (top panels, bar: 50 µm) and confocal fluorescence microscopy images (middle, bottom panels, bar: 20 µm) of EpC40-siAnxA1 cells seeded into collagen gels and treated for 4 days with the pharmacological inhibitors used in this study except pan Jak-inhibitor-I and Tyk2 inhibitor AG1 (see main text, Fig. 6C-F). Note cytoplasmic E-cadherin- and cortical β-actin staining and strong reduction of Vimentin staining upon treatment with a MEK-inhibitor, but little effect of the other inhibitors including the TGFβRI-inhibitor, in contrast to results obtained with EpRasXT cells (see Fig. S6). **C)** Bright field images of EpC40-siAnxA1 cells cultivated in collagen gels and treated with Ras and PI3K inhibitor, respectively for 4 days. Note the clear induction of cell death which supports the dependency of EMT caused by AnxA1 knockdown on Ras and especially on anti-apoptotic PI3K signaling.

Supplemental Figure S6: ***Phenotypical responses of EpRasXT cells to pharmacological inhibitors of EMT-associated signalling pathways***

A) EpRasXT cells cultivated in 3D collagen gels were allowed to form structures for 2 days and then treated with different pharmacological inhibitors for 5 days. Shown are bright field images taken after 7 days of collagen culture (top panels, bar: 100 µm) and confocal immunofluorescence images (middle and bottom panels, bar: 50 µm) of E-cadherin- and Vimentin (red) plus β-actin (green). The MEK inhibitor PD98.059 induced a complete reversion into compact, branched structures with plasma membrane expression of E-cadherin and β-Actin, and little or no Vimentin expression. The TGFβRI-inhibitor only partially reversed the fibroblastoid morphology of EpRasXT cells but showed marked upregulation of plasma membrane E-cadherin, partial cortical localization of β-actin and strong suppression of Vimentin expression (in contrast to its weak effect

on EpC40-siAnxA1 cells; see Fig. S5). **B)** EpRasXT were cultivated in collagen gels and treated or not treated with the Tyk2 inhibitor AG1 as described in panel (**A**). Note induction of cytoplasmic E-cadherin and partial suppression of Vimentin, in contrast to the complete reversal of EMT caused by AG1 in EpC40-siAnxA1 cells.

Supplemental Figure S7: ***Knockdown of AnxA1 causes accumulation of cell-surface EGFR, but EGFR kinase activity is not essential for EMT***

A), B) Analysis of EGF-receptor (EGFR) localized at the cell surface of EpRas- and EpC40 cells before and after siRNA-mediated AnxA1 knockdown, as determined by immunoprecipitation analysis of cell surface biotinylated proteins (**A**) and by the Non Permeant cellular ELISA (**B,** see Supp. Exp. Proc.**)**. Data are shown in comparison to expression of pY- and total EGFR analyzed by WB and for EGFR-biosynthesis rate by immunoprecipitation using [^{35}S]-pulse-labelled cells (for details see Suppl. Exp. Proc.). Positive control in (**B**): EpRasXT cells. **C)** The same cell types as in (**A)** were cultivated as described in Fig. S5A but treated with the EGFR-kinase inhibitor H14 for 2 days. WB analysis for activated (pErk1/2) and total Erk1/2 shows that Erk1/2 phosphorylation is not affected by H14 (due to hyperactivation of the Erk/MAPK pathway; Janda et al, 2002a) but completely inhibited in EpC40-sicontrol cells (Erk/MAPK signalling not hyperactive), while pErk1/2 is not reduced by H14 in EpC40-siAnxA1 cells, suggesting that knockdown of AnxA1 activates Erk1/2 in an EGFR-independent fashion. **D), E)** EpC40-sicontrol and EpC40-siAnxA1 cells were treated with the EGFR kinase inhibitor H14 in collagen gels. Bright field images (**D**) reveal no obvious effect of EGFR-tyrosine kinase inhibition. Similarly, no clear effects of H14 were observed after staining the collagen gels for EMT markers (**E**). This was also true for EpRasXT cells (**E**), suggesting that EGFR-signaling is not involved in Ras/TGFβ and Ras/AnxA1-RNAi induced EMT.

Supplemental Figure S8: ***The breast cancer stem cell targeting drug salinomycin weakly affects Ras/AnxA1-RNAi-induced EMT, but reverses Ras/TGFβ-induced EMT***

A) EpC40-sicontrol and EpC40-siAnxA1 cells were seeded on porous supports and treated after 24 hours with 5 μM salinomycin for 5 days. Confocal immunofluorescence images revealed, however, that Salinomycin induced re-expression of mostly cytoplasmic, but also plasma membrane E-cadherin, partially delocalized ZO-1 and caused partially cortical β-actin localization, but did not

affect high Vimentin and Fibronectin expression (bar 20 µm). **B)** MDCK-DDRafER cells induced to undergo complete EMT upon treatment with Estradiol (E2) and TGFβ after seeding on porous supports were treated or not treated with 6 µM Salinomycin for 5 days, starting 2 days after seeding. Salinomycin completely prevented EMT induction seen without inhibitor (see Fig. S9, bottom), the cells expressing plasma membrane E-cadherin, cortical β-actin, no Fibronectin and little Vimentin, similar as untreated control cells (bars 20 µm).

Supplemental Figure S9: ***EMT induction in MDCK-DDRafER cells by estradiol and TGFβ***

MDCK-DDRafER cells are indistinguishable from MDCK control cells with respect to their polarized epithelial phenotype. They show a typical, epithelial morphology in phase contrast (inset, green frame). Confocal immunofluorescence images (Bar 20 µm, in insets 10 µm) show that the cells express strictly plasma membrane localized E-cadherin and ZO-1, which fully colocalize with cortical β-actin. In contrast, these cells essentially lack Vimentin and Fibronectin. When induced to undergo EMT in response to estradiol (E2) and TGFβ, they form multilayers of fibroblastoid cells, which lack E-cadherin and ZO-1, show β-actin localizing to stress fibers or the cytoplasm, and strongly express Vimentin and Fibronectin (for details of EMT-induction see Suppl. Exp. Proc.).

Supplemental Figure S10: ***Explanatory schemes of the cell- and tissue systems employed***

This scheme depicts the various cellular models used to analyze **A)** endogenous AnxA1 expression in murine and human tumor cells and tissues, and **B)** cellular models to study phenotypic changes induced by knockdown (RNAi) or exogenous expression of AnxA1. The different models and test systems are shown in numbered subpanels (panels A1-A7; panels B1-B4) and are referred to in the text as e.g. Fig. S10A-2. The scheme should be used together with the detailed description of the various cell models in Suppl. Exp. Proc., where the parental normal epithelial cell line EpH4 (used to derive systems A1, A2, B1, B2) and the various EpH4 derivatives and other cell systems used are described. The names of the various cell types shown within a given subpanel have not been inserted into the schemes, but are explained in Suppl. Exp. Proc., e.g. EpRas cells after TGFβ treatment (EpRasXT cells; see subpanel S10A-1). The other cell systems used (see A3, A4, B3, B4) are also explained in detail in Suppl. Exp. Proc., in which we also describe the sources and processing of the tumor samples and databases referred to in panels A5, A6, A7. The symbols for epithelial and mesenchymal markers used in the cartoons and the circular arrow depicting autocrine

TGFβ are explained at the bottom of the figure. EMT, epithelial-mesenchymal transition; red cross, AnxA1 knockdown via RNAi. Differently colored nuclei depict exogenous expression of various, defined genes of interest.

Suppl. Figure S1

A)

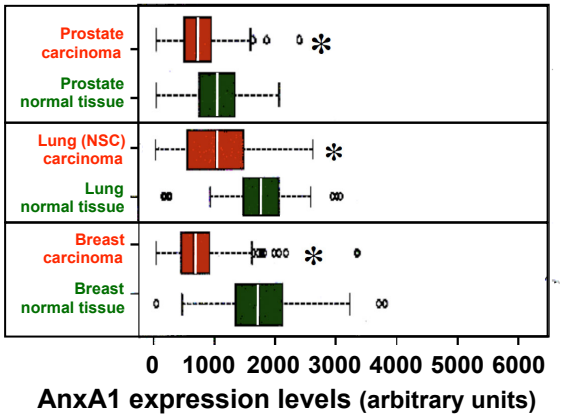

B)

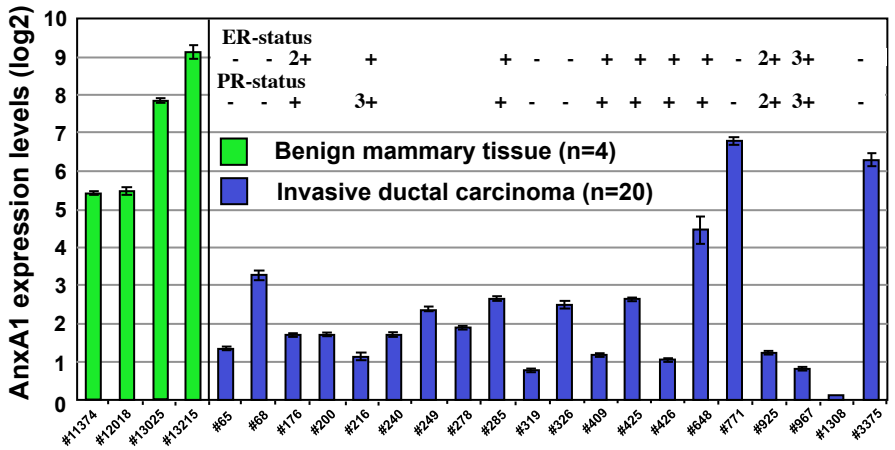

Suppl. Figure S2

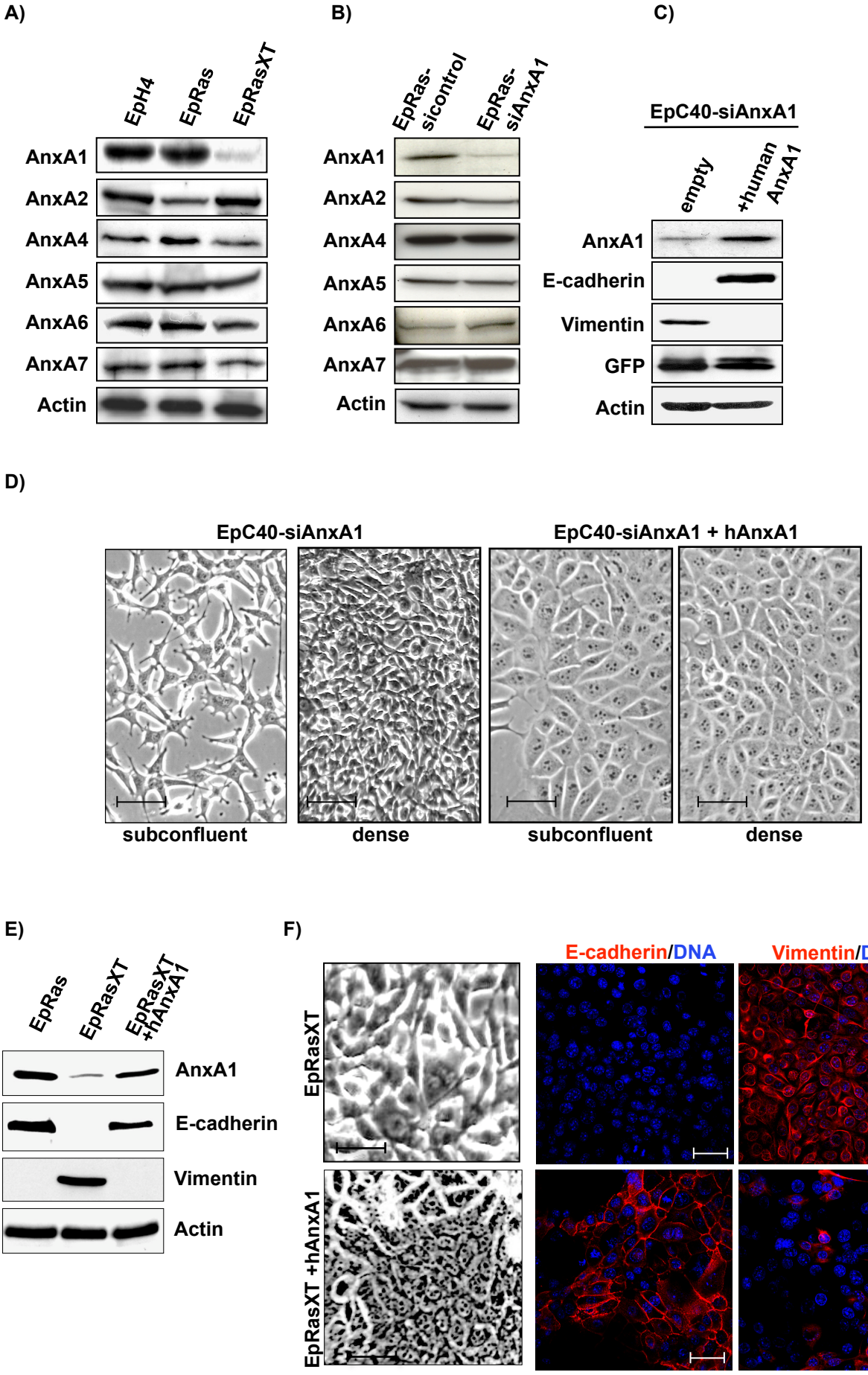

Suppl. Figure S3

A)

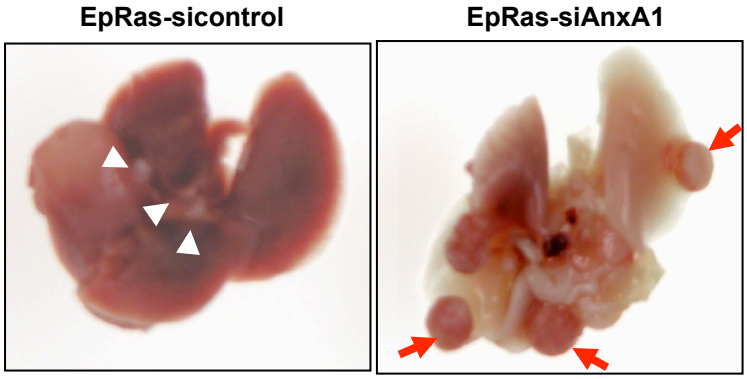

B) Tumor formation (n = 2; 3 injectionsites per mouse)

		control	siAnxA1
HMEC + T + t		-	-
HMEC + T	+ Ras V12	-	+
HMEC + T + t	+ Ras V12	+	ND

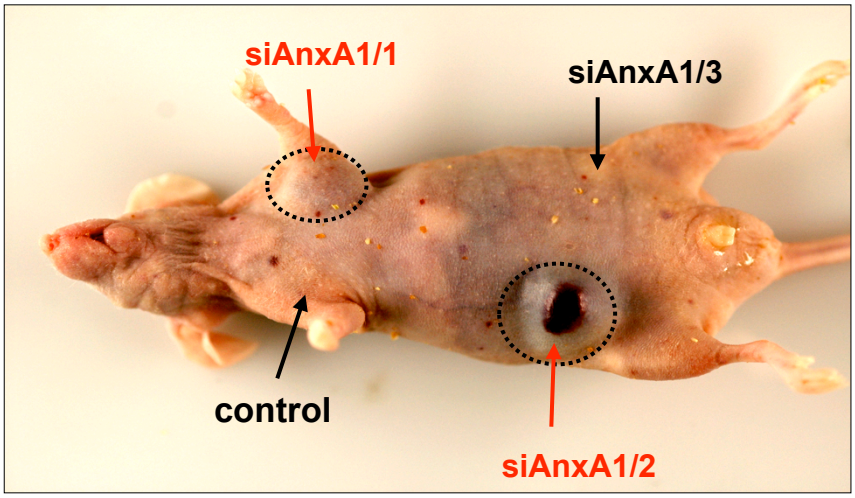

Suppl. Figure S4

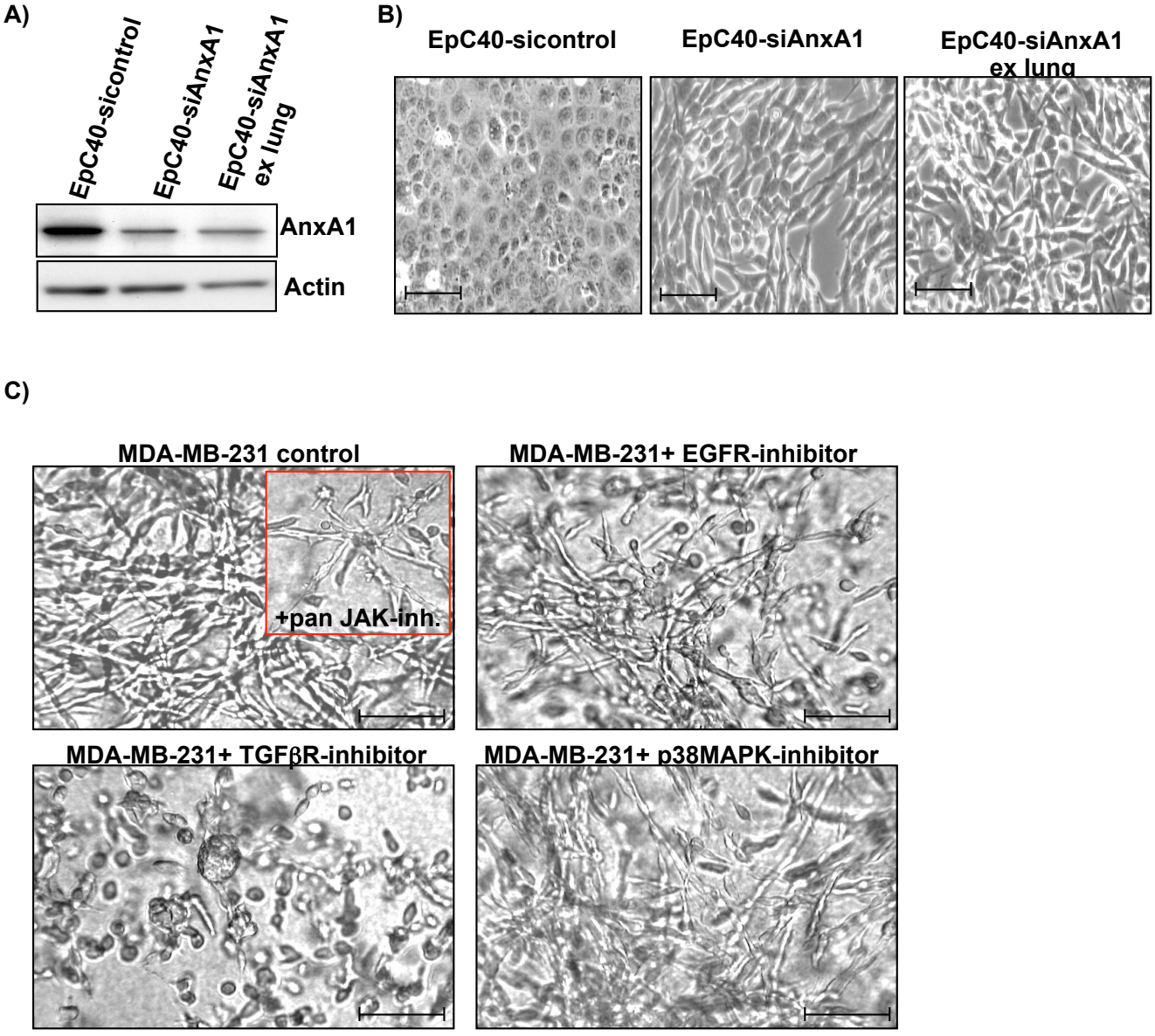

Suppl. Figure S5

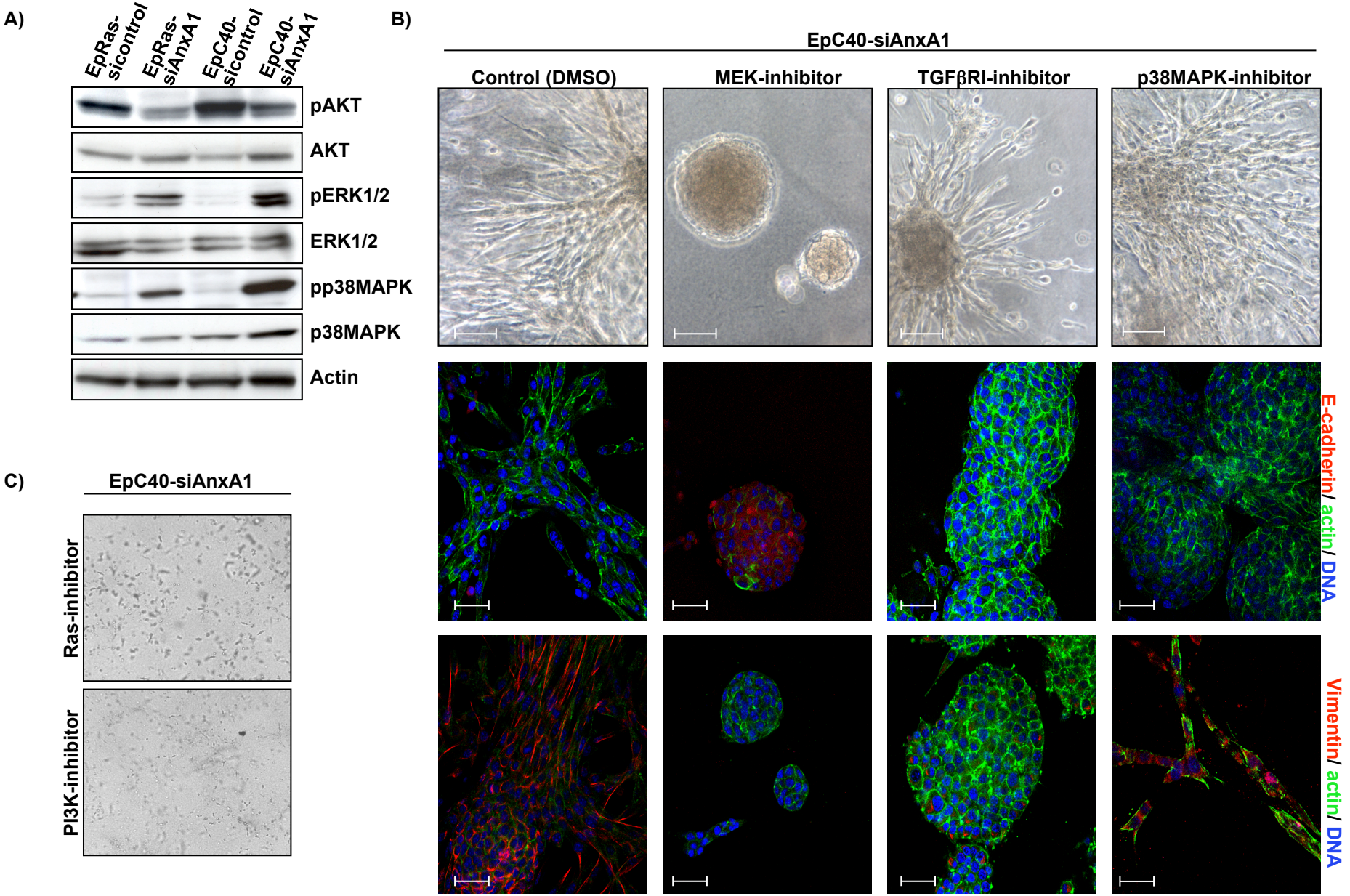

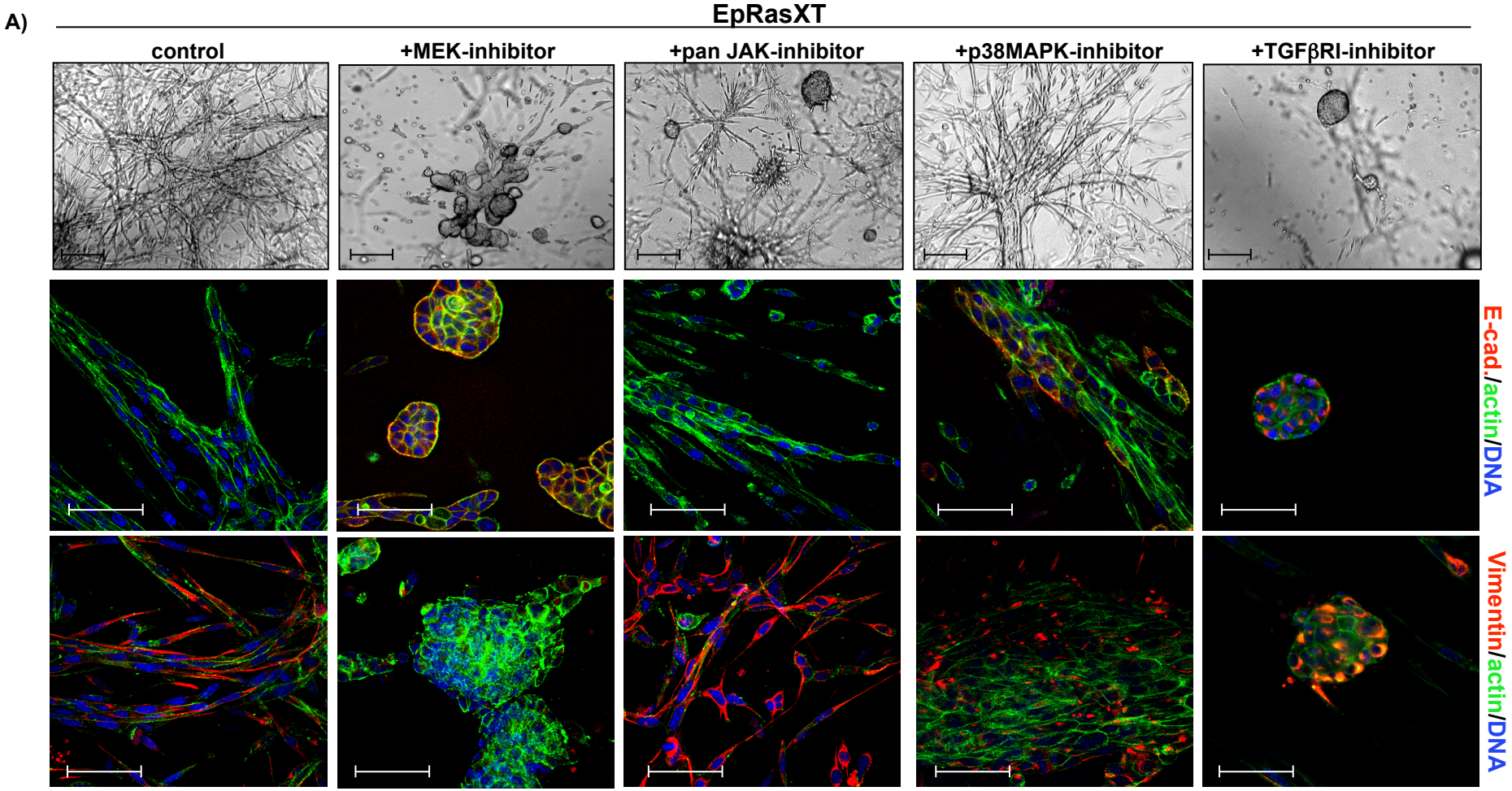

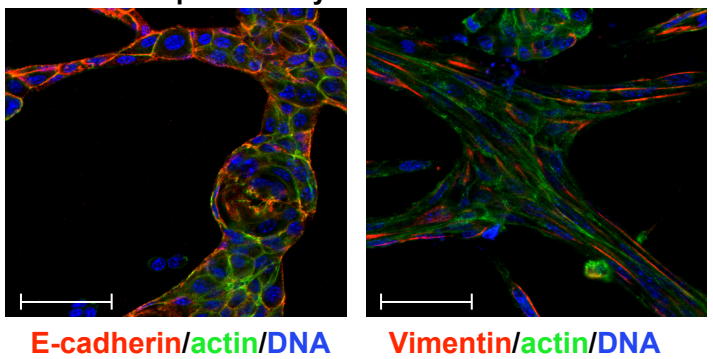

Suppl. Figure S6

Suppl. Figure S7

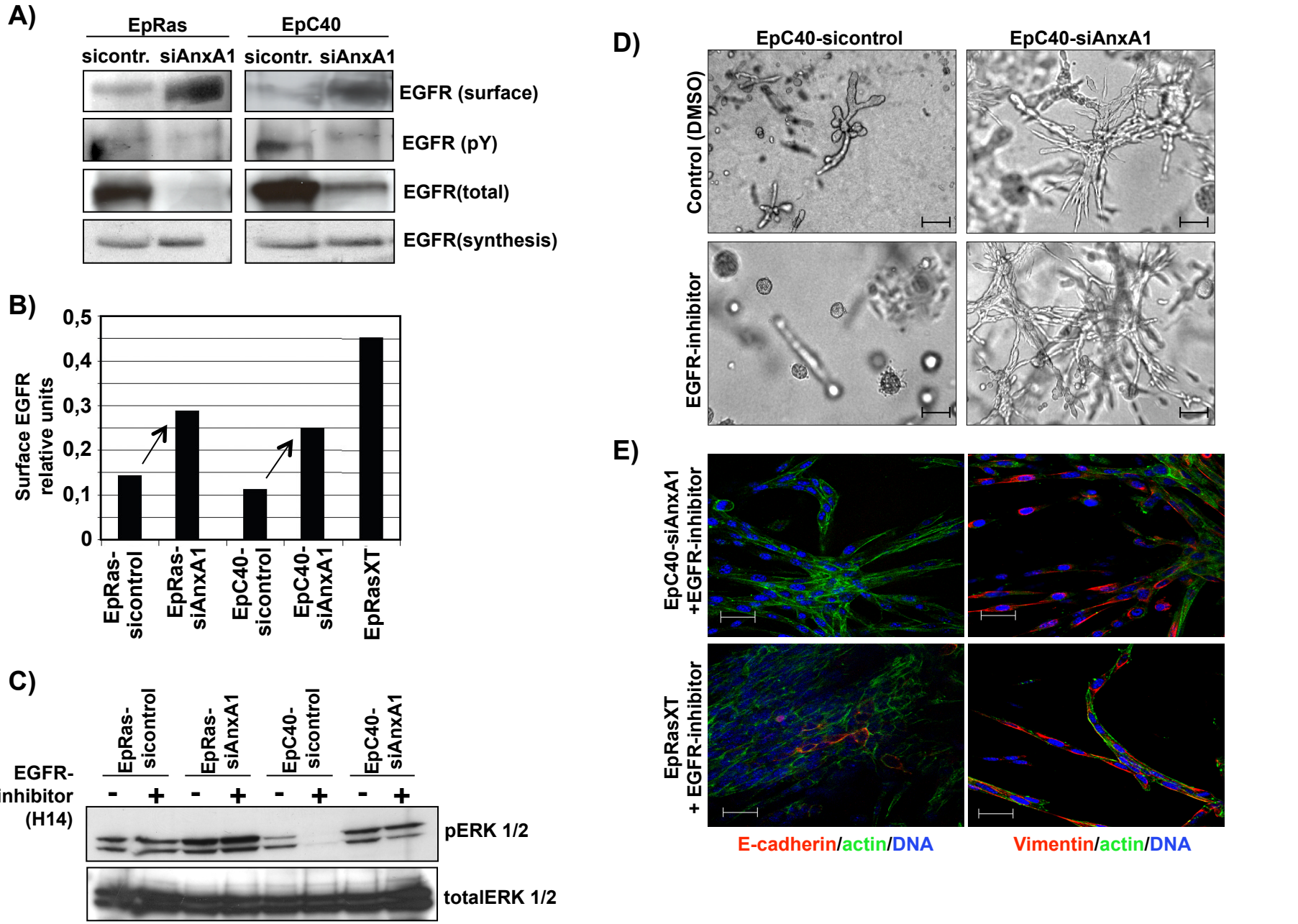

Suppl. Fig S8

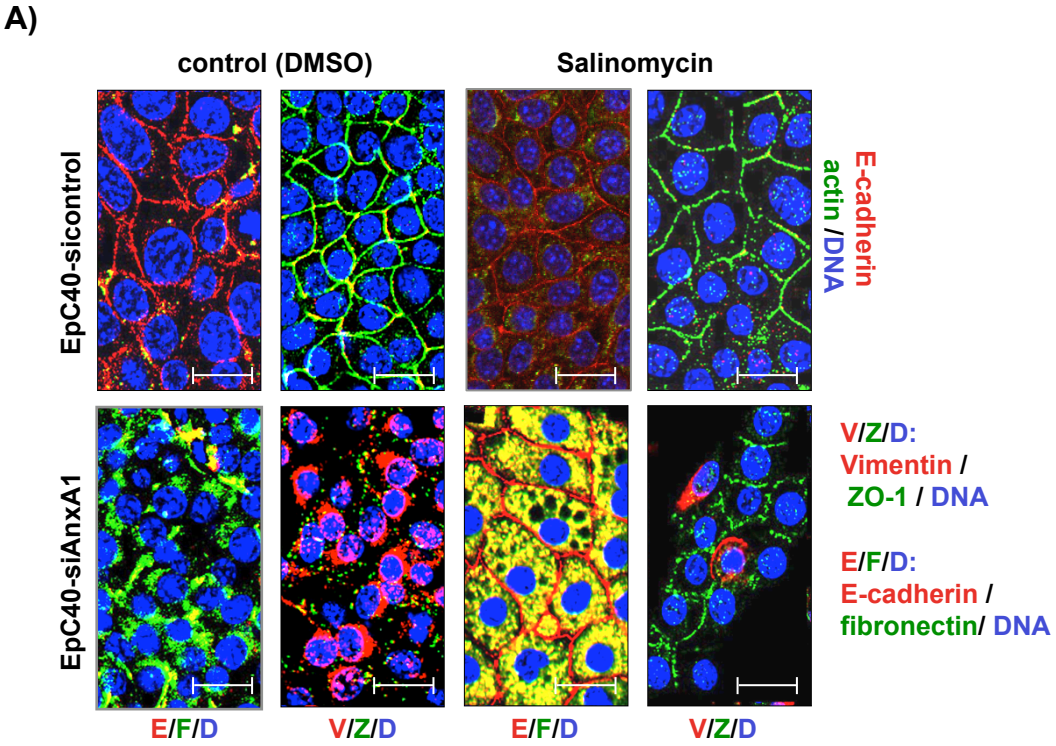
A)
control (DMSO)
Salinomycin
EpC40-sicontrol
EpC40-siAnxA1
E-cadherin
actin /DNA
V/Z/D:
Vimentin /
ZO-1 / DNA
E/F/D:
E-cadherin /
fibronectin/ DNA
E/F/D
V/Z/D
E/F/D
V/Z/D
B)
MDCK-DDRafER (+E2+TGFβ1)
control (DMSO)
Salinomycin
E/A/D:
E-cadherin /
actin / DNA
V/F/D:
Vimentin /
Fibronectin /
DNA
E/A/D
V/F/D
E/A/D
V/F/D

Suppl. Figure S9

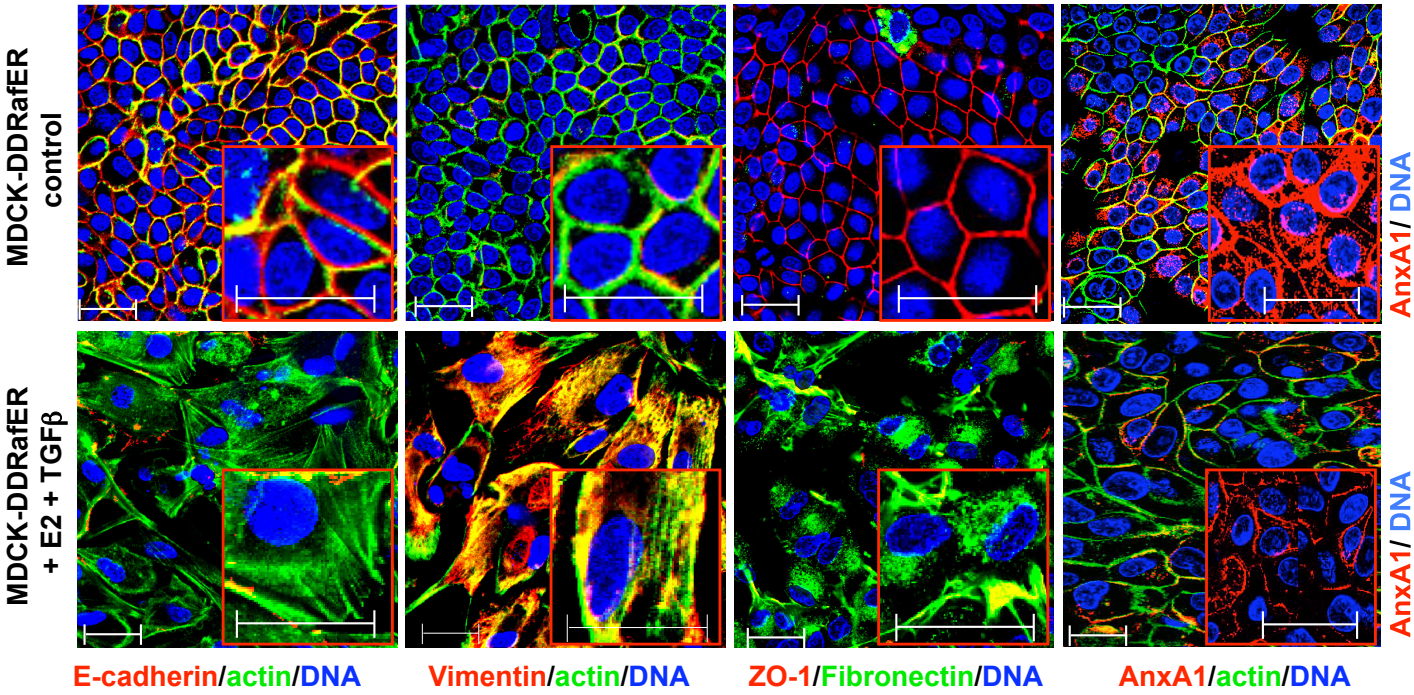

Suppl. Figure S10

A) Models for analyzing endogenous AnxA1 expression:

1. EpRas

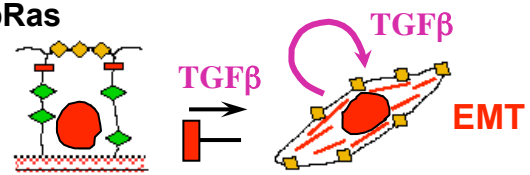

Oncogenic Ha-Ras-V12 hyperactive MAPK/PI3K

2. EpFosER

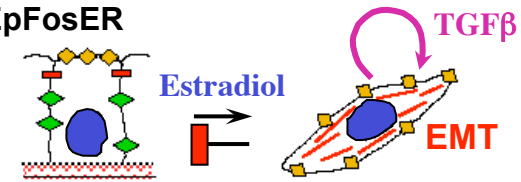

c-Fos-estrogen receptor fusion, EpFosER; autocrine TGFβ1

3. Mouse tumors

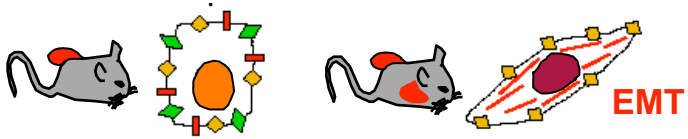

MMTV-Neu-transgenic tumors, late metastasis

MMTV-*Neu* / MMTV-*TGFβ1* transgenic tumor, early metastasis

4. Human mammary carcinoma lines

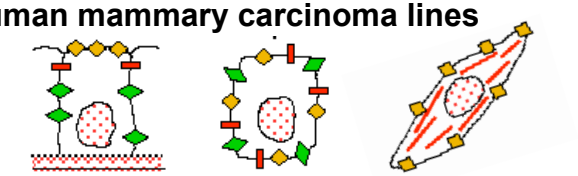

Human "normal"mammary epithelial cells, different mammary carcinoma cell lines: (epitheloid, partial dedifferentiated, EMT)

5. Human normal/tumor-tissue, Affymetrix data base (Gene Logics®), 20-80 tissue samples per normal tissue- or carcinoma type) Chip hybridization.

6. 20 human mammary IDC (invasive ductal carcinoma) samples, 4 normal mammary tissue samples. Quantitative RT-PCR

7. two human breast cancer tissue arrays from 141 patients (TA2, 50; TA3, 91)

B) Cellular models for manipulating AnxA1 protein levels:

1. EpRas

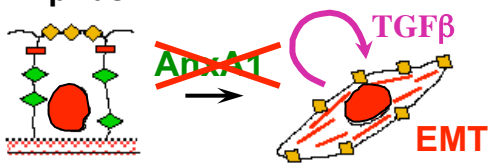

Oncogenic Ha-Ras, no exogenous TGFβ, AnxA1 knockdown induces EMT

2. EpC40

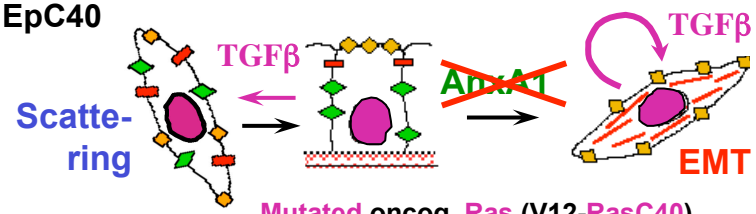

Mutated oncog. Ras (V12-RasC40), hyperactive PI3K, apoptosis protected

3. MDA-MB-231

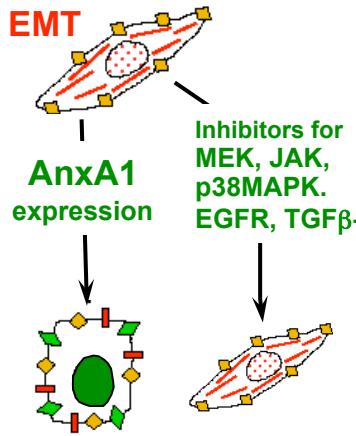

4. HMECs (hP-tert immortalized human mammary epitelial cells) carrying defined oncogenes:

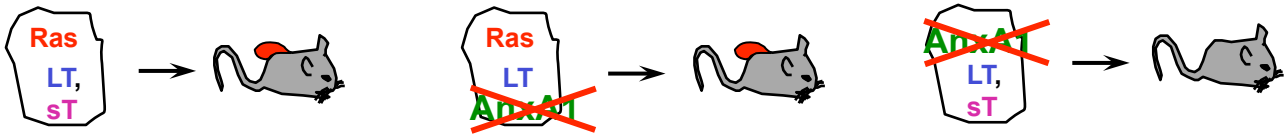

Apical markers (Muc-1, DPP-IV)

Basolateral markers (E-cadherin, actin ring)

Mesenchymal markers (vimentin, N-cadherin, Actin in stress fibers)

Autocrine factors, e.g. TGFβ